

This is an Open Access document downloaded from ORCA, Cardiff University's institutional repository: <https://orca.cardiff.ac.uk/id/eprint/92805/>

This is the author's version of a work that was submitted to / accepted for publication.

Citation for final published version:

Xiang, Pan, Zhao, Yan, Lin, Jiahao, Kennedy, David and Williams, Fred W. 2016. Random vibration analysis for coupled vehicle-track systems with uncertain parameters. *Engineering Computations* 33 (2) , pp. 443-464. 10.1108/EC-01-2015-0009

Publishers page: <http://dx.doi.org/10.1108/EC-01-2015-0009>

Please note:

Changes made as a result of publishing processes such as copy-editing, formatting and page numbers may not be reflected in this version. For the definitive version of this publication, please refer to the published source. You are advised to consult the publisher's version if you wish to cite this paper.

This version is being made available in accordance with publisher policies. See <http://orca.cf.ac.uk/policies.html> for usage policies. Copyright and moral rights for publications made available in ORCA are retained by the copyright holders.



1 **Random vibration analysis for coupled vehicle-track**  
2 **systems with parameter uncertainties based on hybrid**  
3 **pseudo excitation-polynomial chaos expansion method**  
4

P. Xiang <sup>a</sup>

Y. Zhao <sup>a,\*</sup>

J.H. Lin <sup>a</sup>

D. Kennedy <sup>b</sup>

F.W. Williams <sup>b</sup>

<sup>a</sup>State Key Laboratory of Structural Analysis for Industrial Equipment, Faculty of Vehicle Engineering and Mechanics, Dalian University of Technology, Dalian 116023, PR China

<sup>b</sup>Cardiff School of Engineering, Cardiff University, Cardiff CF24 3AA, Wales, UK

\*Corresponding author email: yzhao@dlut.edu.cn

### **Abstract**

This paper proposes a new random vibration-based assessment method for coupled vehicle-track systems with uncertain parameters when subjected to random track irregularity. The vehicle system is simplified to a spring-mass-damper model defined by physical coordinates, while the uncertainties of the vehicle parameters are described as bounded random variables. The track is regarded as an infinite periodic structure, and the dynamic equations of the coupled vehicle-track system, under mixed physical coordinates and symplectic dual coordinates, are established through wheel-rail coupling relationships. The random track irregularities at the wheel-rail contact points are converted to a series of deterministic harmonic excitations with phase lag by using the pseudo excitation method (PEM). Based on the polynomial chaos expansion of the pseudo response, a new chaos expanded pseudo equation is derived, leading to the combined hybrid pseudo excitation method - polynomial chaos expansion (PEM-PCE) method which can efficiently assess the impact of uncertainty propagation on the random vibration analysis. The proposed method is compared with Monte Carlo simulations and good agreement was achieved. It is an effective means for random vibration analysis of uncertain coupled vehicle-track system and has good engineering practicality.

### **Keywords**

Uncertainty; Vehicle-track coupled systems; Polynomial chaos expansion; Pseudo excitation method; Symplectic

## 1 **1 Introduction**

2 There are many uncertainties in practical train structures due to inaccurate processing and  
3 manufacture and so a deterministic model is only an approximation of the real structure. In order  
4 to achieve more reliable predictions for the dynamic behavior of trains and their relationship to the  
5 railway lines, it is necessary to consider the system uncertainties and to develop a method for  
6 predicting their propagation in the coupled system. Over the last decade, this topic has received  
7 increasing attention. (D'Aveni *et al.*, 1996) established an analytical method for a simply  
8 supported beam with uncertain damping ratio and elastic modulus subjected to a deterministic  
9 excitation. Their work included the expansion of the uncertain quantities by a perturbation  
10 technique, together with the evaluation of the transition matrix of the stochastic system.  
11 (Muscolino *et al.*, 2002) concentrated on the problem of calculating the random response of a  
12 distributed parameter system subjected to a moving oscillator with uncertain mass, velocity and  
13 acceleration. (Chang *et al.*, 2006) investigated the dynamic response of a fixed-fixed beam with an  
14 internal hinge on an elastic foundation when it was subjected to an uncertain moving oscillator  
15 (*e.g.* random mass, stiffness, damping and acceleration) and a set of approximate governing  
16 equations of motion were developed using modal analysis and Galerkin's method. They  
17 subsequently adopted an improved perturbation technique in order to evaluate the statistical  
18 responses of the beam. (Gladysz and Śniady, 2009) carried out a power spectral analysis for a  
19 beam with uncertain parameters subjected to a moving force that was assumed to be modeled as a  
20 filtered Poisson process, on the assumption that the natural frequencies of the structure were  
21 uncertain and were modeled by fuzzy numbers, random variables or fuzzy random variables.  
22 General solutions for the spectral density were obtained using a modal dynamic influence function.  
23 (Wu and Law, 2010; 2011) investigated the interaction of uncertain vehicle-bridge systems, with  
24 the bridge modeled as a simply supported Euler-Bernoulli beam with non-Gaussian material  
25 parameters, while the vehicle was modeled by a four degree of freedom mass-spring system. The  
26 road surface roughness was assumed to be a Gaussian random process; the non-Gaussian  
27 uncertainty was handled by means of the Spectral Stochastic Finite Element (SSFE) and the  
28 equations of the vehicle-bridge system were solved using the Newmark method, with suggested  
29 order for both Polynomial Chaos and threshold for truncation in the Karhunen–Loève expansion.

30 The polynomial chaos expansion (PCE) method, as a non-sampling method, has been widely  
31 used to investigate various uncertain problems. This method was first presented by (Wiener, 1938)  
32 based on homogeneous chaos theory. According to the theorem of (Cameron and Martin, 1947),  
33 the homogeneous chaos expansion converges to any stochastic process with finite second-order  
34 moments, which provides a means for Hermitian polynomials to represent the stochastic process.  
35 In the field of structural dynamics, (Ghanem *et al.*, 1991) presented a spectrum approach for  
36 solution of stochastic mechanics by combining Hermitian chaos and finite element method. In a  
37 series of subsequent developments, (Ghanem and Kruger, 1996; Ghanem and Red-Horse, 1999)  
38 have further promoted research in uncertain structural dynamics. Hermitian polynomials are aimed  
39 at Gaussian distribution parameters and are subject to some limitations in applications. Therefore,  
40 (Xiu and Karniadakis, 2002; 2010) developed the generalized polynomial chaos (gPC) method (*i.e.*  
41 the Wiener-Askey scheme), by means of which the optimal convergence polynomials were given  
42 according to different probability distributions, and an efficient stochastic collocation method was  
43 developed to overcome the difficulty caused by multiple variables. In the field of vehicle  
44 dynamics, (Kewlani *et al.*, 2012) investigated the random dynamic behavior of 3-D vehicles

1 moving on an uneven surface, establishing an evaluation method for system responses based on  
2 the gPC method combined with the efficient collocation method (ECM). The experimental results  
3 and numerical simulation well justified this approach.

4 The pseudo excitation method (PEM) is a well-established algorithm for analyzing the responses  
5 of deterministic systems under stationary or non-stationary random excitations (Lin *et al.*, 1992;  
6 2001; 2011; 2014). Because of its simplicity and high efficiency, PEM has been widely used in  
7 many engineering fields (Caprani, 2014; Lin *et al.*, 2014; Yu, 2010; Zhang and Xu, 1999; Zhang *et*  
8 *al.*, 2010). The problem under consideration in this paper is a double-random problem, in that it  
9 deals with a system with uncertainty subjected to random excitations. The parameters of the  
10 coupled vehicle-track system are uncertain, and are characterized as random variables with an arch  
11 probability distribution. Therefore Chebyshev polynomials are the optimal selection for the  
12 orthogonal basis function of which the weight function is equal to the probability density function  
13 (PDF) of the random variable. The track irregularities, as the excitations acting to the system, are  
14 regarded as the spatial random process. The uncertainty of the structural parameters and the  
15 randomness of the excitations are handled in different ways by the proposed PEM-PCE method.  
16 By using PEM in this paper, the track irregularities are converted to harmonic pseudo excitations  
17 and then only the harmonic pseudo governing equation needs to be solved. The Galerkin method  
18 is used to produce the polynomial chaos expansion coefficients of the pseudo responses. To reduce  
19 the dimension of the governing equation, the state equation of a typical substructure is established  
20 in the Hamiltonian space using the symplectic method according to the periodicity of the track  
21 substructures, so that only typical sub-structures need be taken into account in the numerical  
22 computations.

23 In this paper we establish an effective assessment method of random vibration analysis for  
24 uncertain coupled vehicle-track systems subjected to track irregularity. In section 2, the principle  
25 and application for uncertain system of PEM was introduced. In section 3, the governing equation  
26 of coupled vehicle-track systems under mixed physical coordinates and symplectic dual  
27 coordinates were established through wheel-rail coupling relationships. In section 4, a hybrid  
28 pseudo excitation - polynomial chaos expansion method (PEM-PCE) is proposed to solve the  
29 random vibration problem of uncertain structures. In the numerical example, a 10 degree of  
30 freedom rigid body vehicle model is adopted. The random vibration behavior of the coupled  
31 system due to different parameters at different velocities is discussed. Comparison with the direct  
32 Monte Carlo simulation shows that the proposed method significantly improves efficiency while  
33 preserving very high accuracy. Hence the results show that the proposed method is very promising  
34 in both the accuracy and efficiency.

## 35 **2 Pseudo excitation method**

### 36 **2.1 Pseudo excitation method for deterministic systems**

37 The equation of motion of a linear deterministic system subjected to a stationary random  
38 excitation  $\mathbf{p}(t)$  is

$$39 \quad \mathbf{m}\ddot{\mathbf{x}}(t) + \mathbf{c}\dot{\mathbf{x}}(t) + \mathbf{k}\mathbf{x}(t) = \mathbf{p}(t) \quad (2.1)$$

40 The form in the frequency domain is

$$41 \quad [(\mathbf{k} - \omega^2\mathbf{m}) + i\omega\mathbf{c}]\mathbf{X}(i\omega) = \mathbf{P}(i\omega) \quad (2.2)$$

42 where  $\mathbf{X}(i\omega)$  and  $\mathbf{P}(i\omega)$  are the Fourier transforms of  $\mathbf{x}(t)$  and  $\mathbf{p}(t)$ , respectively;  $i$  is the  
43

1 imaginary unit.

2 The response can be expressed as

$$3 \quad \mathbf{X}(i\omega) = \mathbf{H}(i\omega)\mathbf{P}(i\omega) \quad (2.3)$$

4 where  $\mathbf{H}(i\omega) = [\mathbf{k} - \omega^2\mathbf{m} + i\omega\mathbf{c}]^{-1}$  is the frequency response matrix.

5 According to conventional random vibration theory, the power spectrum density function of  
6 response  $\mathbf{S}_x(i\omega)$  can be obtained (Clough and Penzien, 1975) from

$$7 \quad \mathbf{S}_x(i\omega) = \mathbf{H}(i\omega)^*\mathbf{S}_p(i\omega)\mathbf{H}(i\omega)^T \quad (2.4)$$

8 where the asterisk denotes complex conjugate, the superscript T denotes transpose;  $\mathbf{S}_p(i\omega)$  is the  
9 power spectral density (PSD) matrix of random excitation  $\mathbf{p}(t)$ .

10 For complicated FEM systems, the computational effort is often unacceptable. In order to  
11 overcome this difficulty, the following pseudo-excitation method (PEM) has been proved very  
12 efficient.

13 Note that  $\mathbf{S}_p(i\omega)$  is an  $n_s$  order Hermitian matrix with rank  $q$ , which can be decomposed as (De  
14 Rosa *et al.*, 2015, Lin *et al.*, 2014)

$$15 \quad \mathbf{S}_p(i\omega) = \sum_{d=1}^q \lambda_d \boldsymbol{\Psi}_d^* \boldsymbol{\Psi}_d^T \quad (q \leq n_s) \quad (2.5)$$

16 where  $\lambda_d$  and  $\boldsymbol{\Psi}_d$  are the eigenvalue and corresponding eigenvector of  $\mathbf{S}_p(i\omega)$ .

17 Constructing the pseudo excitations

$$18 \quad \tilde{\mathbf{P}}_d(i\omega) = \sqrt{\lambda_d} \boldsymbol{\Psi}_d e^{i\omega t} \quad (d = 1, 2, \dots, q) \quad (2.6)$$

19 Substitute (2.6) for  $\tilde{\mathbf{P}}(t)$  in Equation (2.3)

$$20 \quad \tilde{\mathbf{X}}_d(i\omega) = \mathbf{H}(i\omega)\tilde{\mathbf{P}}_d(i\omega) \quad (2.7)$$

21 where  $\tilde{\mathbf{X}}_d(i\omega)$  is called pseudo response. Clearly,

$$22 \quad \tilde{\mathbf{X}}_d^* \tilde{\mathbf{X}}_d^T = \mathbf{H}(i\omega)^* \lambda_d \boldsymbol{\Psi}_d^* \boldsymbol{\Psi}_d^T \mathbf{H}(i\omega)^T \quad (2.8)$$

23 According to Equation (2.4) and (2.5), one obtains

$$24 \quad \sum_{d=1}^q \tilde{\mathbf{X}}_d^* \tilde{\mathbf{X}}_d^T = \mathbf{H}(i\omega)^* \mathbf{S}_p(i\omega) \mathbf{H}(i\omega)^T = \mathbf{S}_x(i\omega) \quad (2.9)$$

25 As a special and important case, when the random excitations at different points are fully  
26 coherent, the PSD matrix can be decomposed as the product of two vectors, *i.e.* only one  $\lambda_d$   
27 equation (2.5) is non-zero, and so  $\mathbf{S}_p(i\omega)$  has the form

$$28 \quad \mathbf{S}_p(i\omega) = \begin{bmatrix} a_1^2 & a_1 a_2 e^{i\omega(t_1-t_2)} & \dots & a_1 a_{n_s} e^{i\omega(t_1-t_{n_s})} \\ a_2 a_1 e^{i\omega(t_2-t_1)} & a_2^2 & \dots & a_2 a_{n_s} e^{i\omega(t_2-t_{n_s})} \\ \vdots & \vdots & \ddots & \vdots \\ a_{n_s} a_1 e^{i\omega(t_{n_s}-t_1)} & a_{n_s} a_2 e^{i\omega(t_{n_s}-t_2)} & \dots & a_{n_s}^2 \end{bmatrix} \mathbf{S}_p(\omega) \quad (2.10)$$

29 where  $a_i$  ( $i = 1, 2, \dots, n_s$ ) represents the strengths at different excitation points, and the pseudo  
30 excitation can be written as

$$31 \quad \tilde{\mathbf{P}}(i\omega) = \mathbf{V} \sqrt{\mathbf{S}_p} e^{i\omega t} \quad (2.11)$$

32 where  $\mathbf{V} = \{a_1 e^{-i\omega t_1}, a_2 e^{-i\omega t_2}, \dots, a_{n_s} e^{-i\omega t_{n_s}}\}^T$ .

33 So the pseudo response is

$$34 \quad \tilde{\mathbf{X}}(i\omega) = \mathbf{H}(i\omega) \mathbf{V} \sqrt{\mathbf{S}_p} e^{i\omega t} \quad (2.12)$$

35 The PSD of  $\mathbf{x}$  can be obtained from

$$36 \quad \mathbf{S}_x(i\omega) = \tilde{\mathbf{X}}^* \tilde{\mathbf{X}}^T \quad (2.13)$$

37 The above are the basic formulae of the PEM for deterministic systems subjected to stationary  
38 random excitations, which are exactly equivalent to Equation (2.4). However the computation is  
39 much more efficient.

1 **2.2 Pseudo excitation method for uncertain system**

2 It is assumed that the randomness of the external load is independent of the uncertainty of the  
 3 parameters, and that the random load is fully characterized by the PSD. So the construction of  
 4 pseudo excitation for uncertain system is the same as that for deterministic system, *i.e.* as derived  
 5 in Section 2.1.

6 In the framework of the PEM, the governing equation of the uncertain system is expressed as

7 
$$[\mathbf{k}(\boldsymbol{\alpha}) - \omega^2 \mathbf{m}(\boldsymbol{\alpha}) + i\omega \mathbf{c}(\boldsymbol{\alpha})] \tilde{\mathbf{X}}(i\omega) = \tilde{\mathbf{P}}(i\omega) \quad (2.14)$$

8 The uncertainties of parameters are characterized in the frequency-response matrix,  $\mathbf{H}(i\omega, \boldsymbol{\alpha})$   
 9 and the pseudo response is

10 
$$\tilde{\mathbf{X}}(i\omega, \boldsymbol{\alpha}) = \mathbf{H}(i\omega, \boldsymbol{\alpha}) \tilde{\mathbf{P}}(i\omega) \quad (2.15)$$

11 Let  $\{\phi_k(\boldsymbol{\alpha})\}_{k=0}^{\infty} \subset \mathbb{P}$  be an orthogonal polynomial space. The pseudo response can be  
 12 expanded in terms of the basis functions

13 
$$\tilde{\mathbf{X}}(i\omega, \boldsymbol{\alpha}) = \boldsymbol{\phi}(\boldsymbol{\alpha}) \hat{\mathbf{x}}(i\omega) \quad (2.16)$$

14 where  $\hat{\mathbf{x}}(i\omega)$  are the coefficients of the basis functions, of which the solution will be derived in  
 15 Section 4.3.

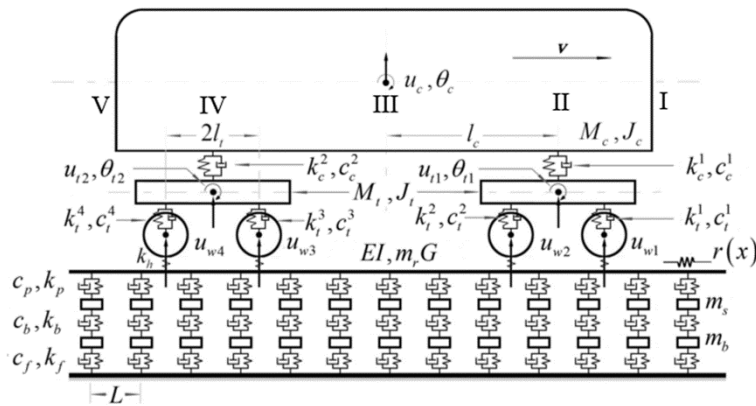
16 By using PEM, the PSD can be expressed as

17 
$$\mathbf{S}_x(i\omega, \boldsymbol{\alpha}) = \tilde{\mathbf{X}}(i\omega, \boldsymbol{\alpha}) \tilde{\mathbf{X}}(i\omega, \boldsymbol{\alpha})^T = \boldsymbol{\phi}(\boldsymbol{\alpha}) \hat{\mathbf{x}}(i\omega) \hat{\mathbf{x}}(i\omega)^T \boldsymbol{\phi}(\boldsymbol{\alpha})^T \quad (2.17)$$

18 **3 Governing equation**

19 The model used for the coupled vehicle-track system is shown in Figure 1 which shows: the  
 20 velocity  $v$  (from left to right); a multi-rigid model for the two-suspension structures of the  
 21 vehicle, the mass of the carriage  $M_c$  and its moment of inertia  $J_c$ ; the half span of the bogie  
 22 spacing  $l_c$ ; the mass of the bogie  $M_t$  and its moment of inertia  $J_t$ ; the half span of the wheel  
 23 spacing  $l_t$ ; the mass of the wheels  $M_w$ ; the primary suspension stiffness and damping  $k_t^i$  and  
 24  $c_t^i$  ( $i = 1,2,3,4$ ); the secondary suspension stiffness and damping  $k_c^i$  and  $c_c^i$  ( $i = 1,2$ ). Figure 1  
 25 also shows how the track is regarded as a three layer structure, comprising the rail, sleepers and  
 26 ballast, with the rail modeled as a single Bernoulli–Euler beam with bending rigidity  $EI$  and  
 27 uniform mass / unit length  $m_r$ ; sleeper and ballast masses of  $m_s$  and  $m_b$ ; rail pad, ballast and  
 28 subgrade stiffnesses of  $k_p$ ,  $k_b$  and  $k_f$ ; and corresponding damping of  $c_p$ ,  $c_b$  and  $c_f$ . A  
 29 linearized spring of stiffness  $k_h = 1.5P_0^{1/3}/G$  connects the wheels to the rail, where  $P_0$  and  $G$ ,  
 30 respectively, represent the static interaction and a connection constant between the wheels and rail  
 31 (Thompson, 1993).

32



33

34

Figure 1: The coupled vehicle-track systems.

### 1 3.1 Equation of motion of the vehicle

2 There are ten degrees of freedom on the model, see Figure 1. These are the vertical and rotational  
 3 motion of the carriage  $(u_c, \theta_c)$  and of its two identical bogies,  $(u_{t1}, \theta_{t1}, u_{t2}, \theta_{t2})$  plus the vertical  
 4 motions of the four rigid wheels  $(u_{w1}, u_{w2}, u_{w3}, u_{w4})$ . The degree of freedom vector used is

$$5 \quad \mathbf{u}_v = \{u_c, \theta_c, u_{t1}, \theta_{t1}, u_{t2}, \theta_{t2}, u_{w1}, u_{w2}, u_{w3}, u_{w4}\}^T \quad (3.1)$$

6 Denoting the  $k$ th component of vector  $\mathbf{u}_v$  by  $u_k$ , the equation of motion of the vehicle, using  
 7 the Lagrange equation, is

$$8 \quad \frac{d}{dt} \left( \frac{\partial T}{\partial \dot{q}_k} \right) - \frac{\partial T}{\partial q_k} + \frac{\partial V}{\partial \dot{q}_k} + \frac{\partial Q}{\partial \dot{q}_k} = 0 \quad (3.2)$$

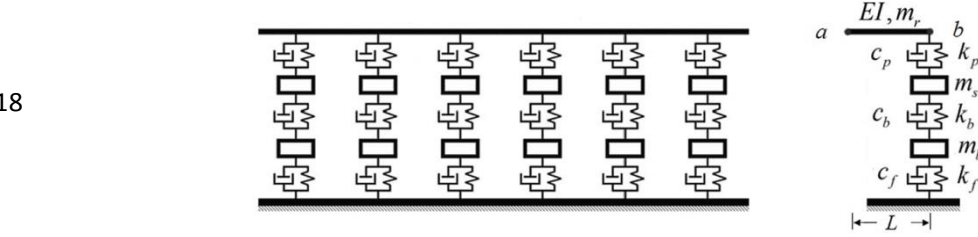
9 where  $T$ ,  $V$  and  $Q$  respectively denote kinetic energy, elastic potential energy and damping  
 10 dissipated energy.

11 Substituting the energy represented by  $\mathbf{u}_v$  into Equation (3.2) gives the equation of motion of the  
 12 vehicle as

$$13 \quad \mathbf{M}_v \ddot{\mathbf{u}}_v + \mathbf{C}_v \dot{\mathbf{u}}_v + \mathbf{K}_v \mathbf{u}_v = \tilde{\mathbf{f}}_v \quad (3.3)$$

14 where  $\mathbf{K}_v$ ,  $\mathbf{M}_v$  and  $\mathbf{C}_v$  are the stiffness, mass and damping matrices of the vehicle and  $\tilde{\mathbf{f}}_v$  is the  
 15 pseudo excitation caused by track irregularity whose specific form will be given by the wheel rail  
 16 relationships in a later section.

### 17 3.2 Equation of motion of the track



19 Figure 2: The periodic arrangement of the elastic track and a typical substructure.

20  
 21 The track is regarded as an infinitely long periodic chain in which the substructure consists of the  
 22 rail between adjacent sleepers, a sleeper and the associated ballast, as shown in Figure 2. The  
 23 equation of motion in the frequency domain of each substructure can then be expressed as

$$24 \quad (\mathbf{K} + i\omega\mathbf{C} - \omega^2\mathbf{M}) \begin{Bmatrix} \mathbf{u}_i^0 \\ \mathbf{u}_a^0 \\ \mathbf{u}_b^0 \end{Bmatrix} = \begin{bmatrix} \mathbf{G}_{ii}^0 & \mathbf{G}_{ia}^0 & \mathbf{G}_{ib}^0 \\ \mathbf{G}_{ai}^0 & \mathbf{G}_{aa}^0 & \mathbf{G}_{ab}^0 \\ \mathbf{G}_{bi}^0 & \mathbf{G}_{ba}^0 & \mathbf{G}_{bb}^0 \end{bmatrix} \begin{Bmatrix} \mathbf{u}_i^0 \\ \mathbf{u}_a^0 \\ \mathbf{u}_b^0 \end{Bmatrix} = \begin{Bmatrix} \mathbf{p}_i^0 \\ \mathbf{p}_a^0 \\ \mathbf{p}_b^0 \end{Bmatrix} \quad (3.4)$$

25 Here  $\mathbf{M}$ ,  $\mathbf{K}$  and  $\mathbf{C}$  are the mass, stiffness and damping matrices of the substructure;  $\mathbf{u}_a^0$  and  
 26  $\mathbf{u}_b^0$  are the displacement vectors at the left and right side interfaces;  $\mathbf{u}_i^0$  is the internal  
 27 displacement vector; and  $\mathbf{p}_a^0$ ,  $\mathbf{p}_b^0$  and  $\mathbf{p}_i^0$  are the corresponding nodal force vectors.

28 Eliminating the internal displacement vector  $\mathbf{u}_i^0$ , Equation (3.4) can be described by the interface  
 29 displacement vectors as

$$30 \quad \begin{bmatrix} \mathbf{G}_{aa} + \mathbf{P}_\beta & \mathbf{G}_{ab} \\ \mathbf{G}_{ba} & \mathbf{G}_{bb} + \mathbf{P}_\alpha \end{bmatrix} \begin{Bmatrix} \mathbf{u}_a \\ \mathbf{u}_b \end{Bmatrix} = \begin{Bmatrix} \mathbf{p}_a^* \\ \mathbf{p}_b^* \end{Bmatrix} \quad (3.5)$$

31 where

1

$$\mathbf{G}_{aa} = \mathbf{G}_{aa}^0 - \mathbf{G}_{ai}^0 [\mathbf{G}_{ii}^0]^{-1} \mathbf{G}_{ia}^0 \quad \mathbf{G}_{ab} = \mathbf{G}_{ab}^0 - \mathbf{G}_{ai}^0 [\mathbf{G}_{ii}^0]^{-1} \mathbf{G}_{ib}^0$$

$$\mathbf{G}_{ba} = [\mathbf{G}_{ab}]^T \quad \mathbf{G}_{bb} = \mathbf{G}_{bb}^0 - \mathbf{G}_{bi}^0 [\mathbf{G}_{ii}^0]^{-1} \mathbf{G}_{ib}^0$$

$$\mathbf{p}_a^* = \mathbf{p}_{ae} - \mathbf{G}_{ai}^0 [\mathbf{G}_{ii}^0]^{-1} \mathbf{p}_{ie} \quad \mathbf{p}_b^* = \mathbf{p}_{be} - \mathbf{G}_{bi}^0 [\mathbf{G}_{ii}^0]^{-1} \mathbf{p}_{ie}$$

2 Here,  $\mathbf{P}_\alpha$  and  $\mathbf{P}_\beta$  are the dynamic stiffness matrices at the two interfaces of the substructure, and  
3  $\mathbf{p}_{ae}$ ,  $\mathbf{p}_{be}$  and  $\mathbf{p}_{ie}$  are the actual external loads.

4 Considering the displacement and force as the state vector, when the substructure has no  
5 external loads (*i.e.*  $\mathbf{p}_{ae} = \mathbf{p}_{be} = \mathbf{p}_{ie} = \mathbf{0}$ ) Equation (3.5) has the following form in state space

$$\begin{Bmatrix} \mathbf{u}_b \\ \mathbf{p}_b \end{Bmatrix} = \begin{bmatrix} \mathbf{S}_{aa} & \mathbf{S}_{ab} \\ \mathbf{S}_{ba} & \mathbf{S}_{bb} \end{bmatrix} \begin{Bmatrix} \mathbf{u}_a \\ \mathbf{p}_a \end{Bmatrix} \quad (3.6)$$

7 where

8

$$\begin{aligned} \mathbf{S}_{aa} &= -[\mathbf{G}_{ab}]^{-1} \mathbf{G}_{aa} & \mathbf{S}_{ab} &= [\mathbf{G}_{ab}]^{-1} \\ \mathbf{S}_{ba} &= -\mathbf{G}_{ba} + \mathbf{G}_{bb} [\mathbf{G}_{ab}]^{-1} \mathbf{G}_{aa} & \mathbf{S}_{bb} &= -\mathbf{G}_{bb} [\mathbf{G}_{ab}]^{-1} \\ \mathbf{p}_a &= -\mathbf{P}_\beta \mathbf{u}_a & \mathbf{p}_b &= -\mathbf{P}_\alpha \mathbf{u}_b \end{aligned}$$

9 Equation (3.6) can be denoted as

10

$$\mathbf{y}_b = \mathbf{S} \mathbf{y}_a \quad (3.7)$$

11 It can be verified that  $\mathbf{S}^{-T} = \mathbf{J} \mathbf{S} \mathbf{J}^{-1}$  or  $\mathbf{S}^T \mathbf{J} \mathbf{S} = \mathbf{J}$ , where  $\mathbf{S}$  is a symplectic matrix which satisfies  
12 the symplectic orthogonality relationships and

13

$$\mathbf{J} = \begin{bmatrix} \mathbf{0} & \mathbf{I}_{n_0} \\ -\mathbf{I}_{n_0} & \mathbf{0} \end{bmatrix} \quad (3.8)$$

14 where  $\mathbf{I}_{n_0}$  is an  $n_0$  order identity matrix;  $n_0$  is the number of degrees of freedom of the  
15 interface.

16 It is known from symplectic mathematical theory that if  $|\mu_i| \leq 1$  is an eigenvalue of  $\mathbf{S}$ , then  
17 so is  $\mu_{n_0+i} = 1/\mu_i$  (Lin *et al.*, 1995). Assume now that  $\mathbf{S}$  has  $2n_0$  eigenvalues and let them be  
18 separated into the following two groups

19

$$\begin{cases} \mu_i & i = 1, 2, \dots, n_0 & |\mu_i| \leq 1 \\ \mu_{n_0+i} = 1/\mu_i & i = 1, 2, \dots, n_0 & |\mu_i| \geq 1 \end{cases} \quad (3.9)$$

20 The corresponding eigenvectors can then be used to constitute the matrix

21

$$\boldsymbol{\Theta} = \{\boldsymbol{\Psi}_1, \boldsymbol{\Psi}_2, \dots, \boldsymbol{\Psi}_{2n_0}\} = \begin{bmatrix} \mathbf{X}_a & \mathbf{X}_b \\ \mathbf{N}_a & \mathbf{N}_b \end{bmatrix} \quad (3.10)$$

22 The state vector  $\mathbf{y}$  can be expanded in terms of the eigenvectors as

23

$$\mathbf{y} = \sum_{i=1}^{2n_0} (a_i \boldsymbol{\Psi}_i + b_i \boldsymbol{\Psi}_{n_0+i}) \quad (3.11)$$

24 The coefficients  $a_i$  and  $b_i$  are rewritten in vector forms  $\mathbf{a}$  and  $\mathbf{b}$ .

25 When the substructure is subjected to a harmonic load, the state vector of the interfaces between  
26 substructures can be obtained by harmonic wave propagation theory as

27

$$\begin{cases} \mathbf{y}_{kr} = \begin{bmatrix} \mathbf{X}_a \\ \mathbf{N}_a \end{bmatrix} \boldsymbol{\mu}^k \mathbf{a} & k \geq 0 \text{ (go right)} \\ \mathbf{y}_{kl} = \begin{bmatrix} \mathbf{X}_b \\ \mathbf{N}_b \end{bmatrix} \boldsymbol{\mu}^{-k} \mathbf{b} & k \leq 0 \text{ (go left)} \end{cases} \quad (3.12)$$

28 Only when  $|\mu_i| = 1$  can the harmonic wave be propagated in the entire substructure chain, and it  
29 is called a pass wave. The remaining harmonic waves decay rapidly away in the propagation, and  
30 are called obstructed waves.

1 When the substructure is subjected to a harmonic excitation, *i.e.*  $k = 0$  in Equation (3.12).

$$2 \quad \begin{Bmatrix} \mathbf{u}_a \\ \mathbf{u}_b \end{Bmatrix} = \begin{bmatrix} \mathbf{X}_b & \mathbf{0} \\ \mathbf{0} & \mathbf{X}_a \end{bmatrix} \begin{Bmatrix} \mathbf{b} \\ \mathbf{a} \end{Bmatrix} \quad (3.13)$$

3 Thus the interface stiffness matrices in Equation (3.5) can be written as

$$4 \quad \mathbf{P}_\alpha = \mathbf{N}_\alpha \mathbf{X}_\alpha^{-1} \quad \mathbf{P}_\beta = -\mathbf{N}_\beta \mathbf{X}_\beta^{-1} \quad (3.14)$$

5 Substituting Equation (3.13) into Equation (3.5) yields the equation of motion denoted by the  
6 symplectic modal coordinate  $\{\mathbf{b}^T, \mathbf{a}^T\}^T$  as

$$7 \quad \begin{bmatrix} \mathbf{G}_{aa} + \mathbf{P}_\beta & \mathbf{G}_{ab} \\ \mathbf{G}_{ba} & \mathbf{G}_{bb} + \mathbf{P}_\alpha \end{bmatrix} \begin{bmatrix} \mathbf{X}_b & \mathbf{0} \\ \mathbf{0} & \mathbf{X}_a \end{bmatrix} \begin{Bmatrix} \mathbf{b} \\ \mathbf{a} \end{Bmatrix} = \begin{Bmatrix} \mathbf{p}_a^* \\ \mathbf{p}_b^* \end{Bmatrix} \quad (3.15)$$

### 8 3.3 Mixed coordinate equations of motion of the coupled vehicle-track

9 In the equation of motion of the vehicle, *i.e.* Equation (3.3),  $\tilde{\mathbf{f}}_v$  can be written as

$$10 \quad \tilde{\mathbf{f}}_v = \{0_{6 \times 1} \quad f_1 \quad f_2 \quad f_3 \quad f_4\}^T \quad (3.16)$$

11 For the  $i$ th substructure subjected to the wheel-rail force, decomposing the force to the  
12 interfaces, Equation (3.15) can be expressed as

$$13 \quad \begin{bmatrix} (\mathbf{G}_{aa} + \mathbf{P}_\beta)\mathbf{X}_b & \mathbf{G}_{ab}\mathbf{X}_a \\ \mathbf{G}_{ba}\mathbf{X}_b & (\mathbf{G}_{bb} + \mathbf{P}_\alpha)\mathbf{X}_a \end{bmatrix} \begin{Bmatrix} \mathbf{b}_i \\ \mathbf{a}_i \end{Bmatrix} = -\mathbf{N}(\xi_i) f_i \quad (i = 1, 2, 3, 4) \quad (3.17)$$

14 where  $\mathbf{N}(\xi)$  is the shape function vector of the Bernoulli-Euler beam element, and  $\xi_i$  is the local  
15 coordinate of the position of the  $i$ th wheel-rail force.

16 Based on the Hertz formula, the interaction between wheels and rails is modeled as a linear spring  
17 connection of stiffness  $k_h$ . Hence the wheel-rail force of the  $i$ th substructure can be expressed as

$$18 \quad f_i = k_h (u_{t_i} - u_{w_i} - r_i) \quad i = 1, 2, 3, 4 \quad (3.18)$$

19 where  $u_{t_i}$  is the displacement of the pair of rails at the  $i$ th contact point,  $u_{w_i}$  is the displacement  
20 and  $r_i$  is the track irregularity.

21 Based on the eigenvector expansion method, the left- and right-hand displacement vectors of the  
22  $i$ th substructure,  $\mathbf{u}_{a,i}$  and  $\mathbf{u}_{b,i}$ , can be obtained as the sum of the responses caused by each of  
23 the four wheel-rail forces, *i.e.*

$$24 \quad \mathbf{u}_{a,i} = \sum_j^4 \mathbf{u}_{a,ji}, \quad \mathbf{u}_{b,i} = \sum_j^4 \mathbf{u}_{b,ji} \quad (3.19)$$

25 where  $\mathbf{u}_{a,ji}$  and  $\mathbf{u}_{b,ji}$  are the left- and right-hand displacement vectors of the  $i$ th substructure  
26 caused by the responses of the  $j$ th substructure.

27 For the displacement of the pair of rails at the contact point, such as the displacement of the  $i$ th  
28 substructure, the contact point  $u_{t_i}$  can be obtained from

$$29 \quad u_{t_i} = \mathbf{N}^T(\xi_i) \begin{Bmatrix} \mathbf{u}_{a,i} \\ \mathbf{u}_{b,i} \end{Bmatrix} \quad (i = 1, 2, 3, 4) \quad (3.20)$$

30 where  $\mathbf{N}(\xi_i)$  is  $i$ th substructure beam element shape function vector.

31 Substituting Equations (3.18)-(3.20) into Equation (3.17), coupling Equations (3.17) and (3.3)  
32 with Equation (3.16) and writing them as a single equation gives the governing equation of the  
33 coupled system as

$$34 \quad \tilde{\mathbf{G}}\tilde{\mathbf{u}} = \tilde{\mathbf{F}} \quad (3.21)$$

35 where

$$\tilde{\mathbf{u}} = \{\mathbf{u}_v^T \quad \mathbf{b}_1^T \quad \mathbf{a}_1^T \quad \mathbf{b}_2^T \quad \mathbf{a}_2^T \quad \mathbf{b}_3^T \quad \mathbf{a}_3^T \quad \mathbf{b}_4^T \quad \mathbf{a}_4^T\} \\ \tilde{\mathbf{F}} = \{0_{6 \times 1}, r_1, r_2, r_3, r_4, \mathbf{N}^T(\xi_1)r_1, \mathbf{N}^T(\xi_2)r_2, \mathbf{N}^T(\xi_3)r_3, \mathbf{N}^T(\xi_4)r_4\}^T$$

36 The specific components of  $\tilde{\mathbf{G}}$  are given as

$$\tilde{\mathbf{G}} = \tilde{\mathbf{G}}_1 + \tilde{\mathbf{G}}_2$$

1 where

$$\begin{aligned} \tilde{\mathbf{G}}_1 &= \text{diag}(\mathbf{G}_v, \mathbf{G}_t, \mathbf{G}_t, \mathbf{G}_t, \mathbf{G}_t), \quad \mathbf{G}_v = \mathbf{K}_v + i\omega\mathbf{C}_v - \omega^2\mathbf{M}_v \\ \tilde{\mathbf{G}}_2 &= \begin{bmatrix} \mathbf{0}_{6 \times 1} & \mathbf{0} & \mathbf{0} \\ \mathbf{0} & -\mathbf{I}_{4 \times 4} & -\tilde{\mathbf{N}}^T\mathbf{W} \\ \mathbf{0} & -\mathbf{N} & \tilde{\mathbf{N}}\tilde{\mathbf{N}}^T\mathbf{W} \end{bmatrix}, \quad \mathbf{G}_t = \begin{bmatrix} (\mathbf{G}_{aa} + \mathbf{P}_\beta)\mathbf{X}_b & \mathbf{G}_{ab}\mathbf{X}_a \\ \mathbf{G}_{ba}\mathbf{X}_b & (\mathbf{G}_{bb} + \mathbf{P}_\alpha)\mathbf{X}_a \end{bmatrix} \\ \tilde{\mathbf{N}} &= \text{diag}(\mathbf{N}(\xi_1), \mathbf{N}(\xi_2), \mathbf{N}(\xi_3), \mathbf{N}(\xi_4)) \end{aligned}$$

2 and

$$\left( \mathbf{w}^{ii} = \begin{bmatrix} \mathbf{X}_b & \mathbf{0} \\ \mathbf{0} & \mathbf{X}_a \end{bmatrix} \right); \left( \mathbf{w}^{ij} = \begin{bmatrix} \mathbf{X}_b \mathbf{u}^{(k_j - k_i)} & \mathbf{0} \\ \mathbf{X}_b \mathbf{u}^{(k_j - k_i - 1)} & \mathbf{0} \end{bmatrix} \right); \left( \mathbf{w}^{ij} = \begin{bmatrix} \mathbf{0} & \mathbf{X}_a \mathbf{u}^{(k_i - k_j - 1)} \\ \mathbf{0} & \mathbf{X}_a \mathbf{u}^{(k_i - k_j)} \end{bmatrix} \right)$$

$i = 1, 2, 3, 4$        $1 \leq i \leq j \leq 4$        $1 \leq j \leq i \leq 4$

3

4

#### 4 Random vibration analysis of the uncertain coupled vehicle-track system

5

6

7

8

Equation (3.21) is the deterministic pseudo governing equation of the coupled vehicle-track system which is established by combining PEM and the symplectic method. In this section, the uncertain parameters are described by a specific PDF, the pseudo response is expanded in polynomial space, and finally the stochastic governing equation is solved by the Galerkin method.

9

#### 4.1 Probabilistic description of the uncertain parameters

10

11

12

13

14

15

16

17

For the vehicle model, it is natural to assume that the uncertain kinetic parameters are random variables obeying some probability distribution. Normal or uniform distributions are commonly used. However, normal distributions of random variables may lead to negative infinite values, which can be meaningless for a physical problem, *e.g.* negative stiffness is not permissible. It is therefore necessary for the system parameters to be bounded. The value of uniform distribution variables is from -1 to 1, which does not cause instability. However for the current problem the system parameters should obey a more concentrated bounded distribution. Therefore, the Wigner semicircle distribution is adopted.

18

Denote the random parameter  $\alpha$  by

19

$$\alpha = \bar{\alpha} + \tilde{\alpha} \quad (4.1)$$

20

21

where  $\bar{\alpha}$  is a deterministic constant and  $\tilde{\alpha}$  is a random variable obeying the Wigner semicircle distribution supported on interval  $[-\kappa, \kappa]$  whose probability density function is

22

$$p(\tilde{\alpha}) = \begin{cases} \frac{2}{\pi\kappa^2} (\kappa^2 - \tilde{\alpha}^2)^{1/2} & |\tilde{\alpha}| \leq \kappa \\ 0 & |\tilde{\alpha}| > \kappa \end{cases} \quad (4.2)$$

23

Calculate the mean and variance of  $\alpha$  as

24

$$E[\alpha] = E[\bar{\alpha} + \tilde{\alpha}] = \bar{\alpha} \quad (4.3)$$

25

$$D[\alpha] = E[(\alpha - \bar{\alpha})^2] = \kappa^2/4 \quad (4.4)$$

26

where  $E[\cdot]$  is the expectation operator.

27

28

#### 4.2 Pseudo excitation for the track irregularity

29

30

31

32

Actual track irregularity is a non-ideal smoothness characteristic of the rail surface caused by many random factors, such as manufacturing and abrasion. For the assumed randomness, the same class of track will have the same probability characteristic everywhere. Hence when a train runs along the track at uniform velocity, the excitation caused by the track irregularity can be regarded

1 as a stationary random process (Garg, 1984; Iwnicki, 2006). It is assumed that the track  
 2 irregularity  $r(x)$  with respect to the space coordinate  $x$  is a zero-mean stationary random  
 3 process with power spectral density function  $S_{rr}(\Omega)$ .

4 Assume that the wheel is in contact with the rail at all times, *i.e.* there is no sliding or derailment.  
 5 The track irregularity can be converted from the space domain  $r(x)$  to the time domain  $r(t)$   
 6 by the relationship  $x = vt$ . This gives a zero-mean stationary random process with respect to the  
 7 time coordinate  $t$ , with the power spectral density function  $S_{rr}(\omega)$  obtained from  $S_{rr}(\Omega)$  as

$$8 \quad S_{rr}(\omega) = (S_{rr}(\Omega))/v, \quad \omega = \Omega v = 2\pi v/\lambda \quad (4.5)$$

9 where  $\lambda$  is the spatial wavelength.

10 The coupled system is subjected to four excitations at the wheel-rail contact points which are all  
 11 from the same source. This fully coherent (multi-phase) random excitation can be regarded as a  
 12 generalized single excitation. The pseudo excitation is constructed as

$$13 \quad \tilde{\mathbf{F}} = \{\mathbf{0}_{6 \times 1}, e^{-i\omega t_1}, e^{-i\omega t_2}, e^{-i\omega t_3}, e^{-i\omega t_4}, \mathbf{N}^T(\xi_1)e^{-i\omega t_1}, \dots \\ 14 \quad \mathbf{N}^T(\xi_2)e^{-i\omega t_2}, \mathbf{N}^T(\xi_3)e^{-i\omega t_3}, \mathbf{N}^T(\xi_4)e^{-i\omega t_4}\}^T \sqrt{S_{rr}(\omega)} e^{i\omega t} \quad (4.6)$$

15 Without loss of generality, it is assumed that  $t_1=0$ , so that  $t_i$  ( $i = 2,3,4$ ) is the time lag between  
 the other excitations and the first excitation.

### 16 4.3 Solution of the stochastic governing equation

17 The stochastic governing equation in frequency domain can be expressed as

$$18 \quad \tilde{\mathbf{G}}(\boldsymbol{\alpha})\tilde{\mathbf{u}} = \tilde{\mathbf{F}} \quad (4.7)$$

19 where

$$20 \quad \tilde{\mathbf{G}}(\boldsymbol{\alpha}) = \bar{\mathbf{G}}_0 + \sum_{i=1}^n \tilde{\alpha}_i \tilde{\mathbf{G}}_i$$

21  $\bar{\mathbf{G}}_0$  and  $\tilde{\mathbf{G}}_i$  ( $i = 1,2, \dots, n$ ) are the mean value matrix and the nominal variance matrix,  
 22 respectively, which are constructed in Equation (3.21);  $\tilde{\alpha}_i$  are independence random variables  
 23 denoted by Equation (4.1) which are the components of the vector  $\boldsymbol{\alpha}$ .

#### 24 4.3.1 Polynomial chaos expansion

25 If we can obtain the pseudo response  $\tilde{\mathbf{u}}$ , the response PSD can be obtained efficiently from  
 26 Equation (2.8). In this section, the pseudo response is expanded in polynomial space to assess the  
 27 uncertainty impact on the power spectrum and spectral moments.

28 From the viewpoint of functional analysis, the dynamic responses of random structures can be  
 29 regarded as the locus of solutions in the function spaces. By selecting the appropriate basis  
 30 function  $\{\varphi_l(\boldsymbol{\alpha})\}_{l=0}^{\infty}$ , the random response  $\tilde{\mathbf{u}}(\boldsymbol{\alpha}, t)$  in Equation (4.7) can be expanded as

$$31 \quad \tilde{\mathbf{u}}(\boldsymbol{\alpha}, t) = \sum_{l=1}^{\infty} \mathbf{x}_l \varphi_l(\boldsymbol{\alpha}) e^{i\omega t} \quad (4.8)$$

32 where  $\mathbf{x}_l$  is the deterministic coefficient vector, which can be understood as the projection of  $\tilde{\mathbf{u}}$   
 33 on the basis functions.

34 Consider now the orthogonal polynomials as basis functions:

$$35 \quad \varphi_l(\boldsymbol{\alpha}) = \prod_{i=1}^n P_{l_i}(\tilde{\alpha}_i) \quad (4.9)$$

36 where,  $P_{l_i}(\tilde{\alpha}_i)$  is the  $l_i$ th orthogonal polynomial of the random variable  $\alpha_i$ . Hypothetically there  
 37 are  $n$  independent random variables and each one has an  $m_i$ -order orthogonal expansion, with  
 38  $0 \leq l_i \leq m_i, 1 \leq l \leq L$  and with  $L = \prod_{i=1}^n (m_i + 1)$  as the number of polynomial basis  
 39 functions.

40 The choice of orthogonal polynomials depends on the probability distribution of the random  
 41 variables, *e.g.* Hermite polynomials for standard normal distribution and Legendre polynomials

1 for uniform distribution. In this work, Chebyshev polynomials (Borwein and Erdelyi, 1995) are  
 2 adopted, whose expression is

$$3 \quad H_n(\tilde{\alpha}) = \sum_{k=0}^{\lfloor n/2 \rfloor} \frac{(-1)^k (n-k)!}{k!(n-2k)!} (2\tilde{\alpha})^{n-2k} \quad (4.10)$$

4 *e.g.* the first three are:

$$5 \quad H_0(\tilde{\alpha}) = 1, H_1(\tilde{\alpha}) = 2\tilde{\alpha}, H_2(\tilde{\alpha}) = 4\tilde{\alpha}^2 - 1, H_3(\tilde{\alpha}) = 8\tilde{\alpha}^3 - 4\tilde{\alpha} \quad (4.11)$$

6 The weight function of the Chebyshev polynomials is  $2/\pi\sqrt{1-\tilde{\alpha}^2}$ . This connects the  
 7 expectation of the random variable from Equation (4.2) and the orthogonality of the polynomials  
 8 giving:

$$9 \quad \text{Orthogonality:} \quad \int_{-1}^1 2/\pi\sqrt{1-\tilde{\alpha}^2} H_m(\tilde{\alpha}) H_n(\tilde{\alpha}) d\tilde{\alpha} = \delta_{mn} \quad (4.12)$$

$$10 \quad \text{Recursiveness:} \quad \tilde{\alpha} H_n(\tilde{\alpha}) = \frac{1}{2} [H_{n-1}(\tilde{\alpha}) + H_{n+1}(\tilde{\alpha})] \quad (4.13)$$

11 According to Equations (4.8) and (4.9),  $\tilde{\mathbf{u}}(\boldsymbol{\alpha}, t)$  can be expanded on the Chebyshev polynomials  
 12 basis function with an appropriate truncation

$$13 \quad \tilde{\mathbf{u}}(\boldsymbol{\alpha}, t) = \left( \sum_{0 \leq l_j \leq m_j} \mathbf{x}_{l_1 l_2 \dots l_n} \prod_{j=1}^n H_{l_j}(\tilde{\alpha}_j) \right) e^{i\omega t} \quad (4.14)$$

14 which can be re-written in the following matrix form to facilitate derivation

$$15 \quad \tilde{\mathbf{u}}(\boldsymbol{\alpha}, t) = \boldsymbol{\Phi}(\boldsymbol{\alpha}) \mathbf{x} e^{i\omega t} \quad (4.15)$$

16 where  $\boldsymbol{\Phi}(\boldsymbol{\alpha})$  is a block diagonal matrix with each diagonal element being  
 17  $\boldsymbol{\varphi}(\boldsymbol{\alpha}) = [\prod_{i=1}^n H_0(\tilde{\alpha}_i), \dots, \prod_{i=1}^n H_m(\tilde{\alpha}_i)]_{1 \times L}$  and  $\mathbf{x}$  is a column vector. Equation (4.15) is a  
 18 pseudo response polynomial chaos expansion model. If the deterministic coefficient vector  $\mathbf{x}$  is  
 19 known, the quantitative assessment of the uncertain impact is achieved by using statistical theory.

### 20 4.3.2 Galerkin method

21 Assume now that the external loads are independent of the vehicle-track system. Substituting  
 22 Equation (4.15) into Equation (4.7), left multiplying by  $\boldsymbol{\Phi}(\boldsymbol{\alpha})^T$  on both sides and calculating the  
 23 expectation to  $\boldsymbol{\alpha}$ , the governing equation for random response prediction is obtained, according to  
 24 Equations (4.12) and (4.13), as

$$25 \quad \mathbf{A}_{\tilde{\mathcal{G}}} \mathbf{x} = \mathbf{b}_{\tilde{\mathcal{F}}} \quad (4.16)$$

26 In order to explain the specific forms of  $\mathbf{A}_{\tilde{\mathcal{G}}}$  and  $\mathbf{b}_{\tilde{\mathcal{F}}}$ ,  $\otimes$  is used to denote the Kronecker-product  
 27 and the three matrices  $\mathbf{T}$ ,  $\mathbf{U}$  and  $\mathbf{E}$  are defined as

$$28 \quad \mathbf{T}_i = \begin{bmatrix} 1 & & & \\ & 1 & & \\ & & \ddots & \\ & & & 1 \end{bmatrix}_{(m_i+1) \times (m_i+1)} \quad \mathbf{U}_i = \begin{bmatrix} 0 & 0.5 & & \\ 0.5 & 0 & \ddots & \\ & \ddots & \ddots & 0.5 \\ & & 0.5 & 0 \end{bmatrix}_{(m_i+1) \times (m_i+1)} \quad \mathbf{E} = \begin{bmatrix} 1 \\ 0 \\ \vdots \\ 0 \end{bmatrix}_{L \times 1}$$

$$29 \quad \text{Hence} \quad \mathbf{A}_{\tilde{\mathcal{G}}} = \mathbf{A}_{\tilde{\mathcal{G}}_0} + \sum_{i=1}^n \mathbf{A}_{\tilde{\mathcal{G}}_i} \quad (4.17)$$

$$30 \quad \mathbf{A}_{\tilde{\mathcal{G}}_0} = \bar{\mathbf{G}}_0 \otimes (\mathbf{T}_1 \otimes \mathbf{T}_2 \otimes \dots \otimes \mathbf{T}_n)$$

$$31 \quad \mathbf{A}_{\tilde{\mathcal{G}}_i} = \tilde{\mathbf{G}}_i \otimes (\mathbf{T}_1 \otimes \mathbf{T}_2 \otimes \dots \otimes \mathbf{U}_i \otimes \dots \otimes \mathbf{T}_n)$$

$$32 \quad \text{and} \quad \mathbf{b}_{\tilde{\mathcal{F}}} = \tilde{\mathbf{F}} \otimes \mathbf{E} \quad (4.18)$$

33 The governing equation given in Equation (4.7) has thus been transformed into the high-order  
 34 deterministic equation given by Equation (4.16), which is easy to solve. When the component  
 35 column vector  $\mathbf{x}$  has been obtained, the response  $\tilde{\mathbf{u}}(\boldsymbol{\alpha}, t)$  can be calculated from Equation (4.15).  
 36 It is obvious that the coefficient matrix of the governing equation Equation (4.16) is sparse, which

1 yields computational savings.

### 2 4.3.3 Statistical assessment

3 Assume that a specified response is concerned and expand it as

$$4 \quad \tilde{u}(\boldsymbol{\alpha}, t) = \boldsymbol{\varphi}(\boldsymbol{\alpha}) \hat{\mathbf{x}} e^{i\omega t} = \sum_{l=1}^L \varphi_l(\boldsymbol{\alpha}) \hat{x}_l e^{i\omega t} \quad (4.19)$$

5 where  $\hat{\mathbf{x}}$  is the projection of the specified response on the basis functions, and is part of the  $\mathbf{x}$   
6 given by Equation (4.16).

7 The PSD and variance can easily be obtained by using PEM, giving

$$8 \quad S_{out}(\boldsymbol{\alpha}, \omega) = (\tilde{u}(\boldsymbol{\alpha}, t))^* (\tilde{u}(\boldsymbol{\alpha}, t))^T = \boldsymbol{\varphi}(\boldsymbol{\alpha}) \hat{\mathbf{x}}^* \hat{\mathbf{x}}^T \boldsymbol{\varphi}(\boldsymbol{\alpha}) \quad (4.20)$$

$$9 \quad \sigma_{out}^2(\boldsymbol{\alpha}) = 2 \int_0^{+\infty} S_{out}(\boldsymbol{\alpha}, \omega) d\omega \quad (4.21)$$

10 The mean of the random vibration power spectrum caused by the uncertain parameters can  
11 found by taking the expectation on Equation (4.20), by using the orthogonality of the polynomials,  
12 as

$$13 \quad \bar{S}_{out} = E[S_{out}(\boldsymbol{\alpha}, \omega)] = E[\boldsymbol{\varphi}(\boldsymbol{\alpha}) \hat{\mathbf{x}}^* \hat{\mathbf{x}}^T \boldsymbol{\varphi}(\boldsymbol{\alpha})] = \sum_{l=1}^L |\hat{x}_l|^2 \quad (4.22)$$

14 where  $|\cdot|$  is the modulo operation. Equation (4.22) shows that the mean of the response PSD of  
15 concern can be obtained by summing up the squares of the modulo of each coefficient, which  
16 yields both very concise expressions and efficient computation.

17 The mean of the response variance of concern is found by

$$18 \quad \bar{\sigma}_{out}^2 = E[\sigma_{out}^2(\boldsymbol{\alpha})] = 2 \int_0^{+\infty} \bar{S}_{out} d\omega \quad (4.23)$$

19 Also, the variance of the response PSD or the variance of concern is found by

$$20 \quad D[S_{out}(\boldsymbol{\alpha}, \omega)] = E[(S_{out} - \bar{S}_{out})^2] \quad (4.24)$$

$$21 \quad D[\bar{\sigma}_{out}^2(\boldsymbol{\alpha}, \omega)] = E[(\sigma_{out}^2 - \bar{\sigma}_{out}^2)^2] \quad (4.25)$$

22 When there are many variables, a multi-dimensional integral operation is needed to calculate the  
23 variance of random vibration response caused by uncertain parameters directly from Equations  
24 (4.24) and (4.25). Unfortunately, unlike for the expectation operation, the variance operation  
25 cannot use the orthogonality of the basis functions. Therefore Monte Carlo method integration is  
26 recommended here because, due to the simple form of the statistical functions, it is highly  
27 efficient.

28

## 29 5 Numerical examples

Vehicle parameters			
Carriage mass $M_c$	$34 \times 10^3 \text{kg}$	Primary damping $c_t$	$12 \times 10^3 \text{Ns/m}$
Carriage inertia $J_c$	$2.277 \times 10^6 \text{m}^4$	Secondary stiffness $k_c$	$800 \times 10^3 \text{N/m}$
Bogie mass $M_t$	3000kg	Secondary damping $c_c$	$160 \times 10^3 \text{Ns/m}$
Bogie inertia $J_t$	$2710 \text{m}^4$	Wheel spacing $2l_t$	2.4m
Wheel mass $M_w$	1400kg	Bogie spacing $2l_c$	18m
Primary stiffness $k_t$	$1100 \times 10^3 \text{N/m}$	Contact constant $G$	$5.135 \times 10^{-8} \text{m/N}^{2/3}$
Track parameters			
Rail bending rigidity $EI$	$13.25 \times 10^6 \text{Nm}^2$	Ballast stiffness $k_b$	$4.8 \times 10^8 \text{N/m}$

Rail linear density $m_r$	121.28kg/m	Subgrade stiffness $k_f$	$13 \times 10^7$ N/m
Sleeper spacing $L$	0.545m	Rail pad damping $c_p$	$7.5 \times 10^4$ Ns/m
Sleeper mass $m_s$	237kg	Ballast damping $c_b$	$5.88 \times 10^4$ Ns/m
Ballast mass $m_b$	1365.2kg	Subgrade damping $c_f$	$3.115 \times 10^4$ Ns/m
Rail pad stiffness $k_p$	$15.6 \times 10^7$ N/m		

1 Table 1 The parameters of vehicle and track

2

3 The parameters of the coupled vehicle-track system were given the values shown in Table 1  
4 (Zhang *et al.*, 2010) and the uncertain parameters are shown in Table 2. From front to rear, there  
5 are five locations, head (I), front spring (II), center (III), rear spring (IV) and stern (V) under  
6 consideration as shown in Figure 1. The PSD of the track irregularity is expressed as:

$$7 \quad S_r(\Omega) = \begin{cases} \frac{0.25 \times 0.0339 \times 0.8245^2}{\Omega^2(\Omega^2 - 0.8245^2)} \text{ (cm}^2/\text{rad/m)} & \text{when } \Omega \leq 2\pi \\ 0.036(\Omega/2\pi)^{-3.15} \text{ (mm}^2/\text{rad/m)} & \text{when } \Omega > 2\pi \end{cases} \quad (5.1)$$

8 where  $\Omega$  is the space circular frequency. The power spectral density function in the time domain  
9 was transformed from  $S_r(\Omega)$  by Equation (4.5).

10

Parameter $\alpha$	Mean $\bar{\alpha}$	Standard deviation $\kappa/2$
Primary stiffness $k_t$	$1100 \times 10^3$ N/m	$220 \times 10^3$ N/m
Primary damping $c_t$	$12 \times 10^3$ Ns/m	$2.4 \times 10^3$ Ns/m
Secondary stiffness $k_c$	$800 \times 10^3$ N/m	$160 \times 10^3$ N/m
Secondary damping $c_c$	$160 \times 10^3$ Ns/m	$32 \times 10^3$ Ns/m
Carriage mass $M_c$	$34 \times 10^3$ kg	$6.8 \times 10^3$ kg
Carriage inertia $J_c$	$2.277 \times 10^6$ m <sup>4</sup>	$4.554 \times 10^5$ m <sup>4</sup>

11 Table 2 Uncertain parameters

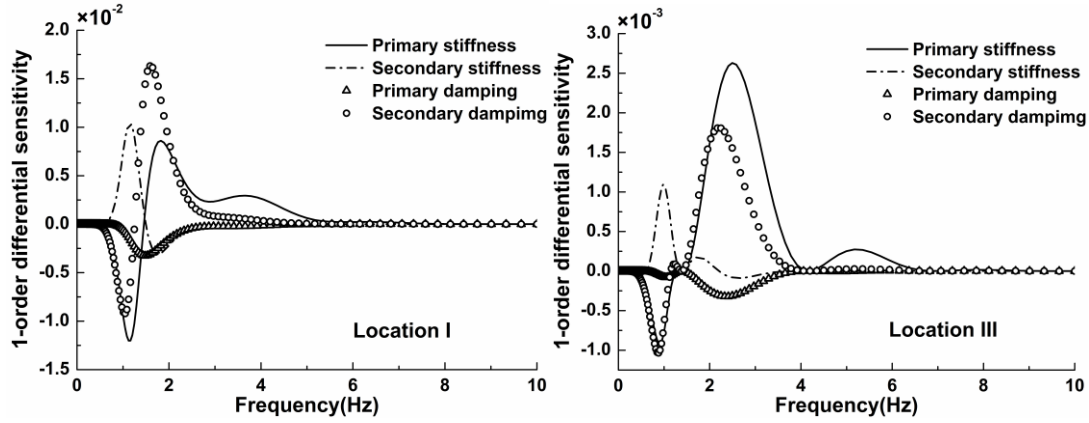
12

### 13 5.1 The kinetic parameter sensitivity analysis of the vehicle system

14 For different kinetic parameters, impacts on any specified response of concern are different. It is a  
15 waste of computing cost to account for all uncertainty of the parameters. So firstly, the important  
16 uncertain parameters were found using response sensitivity analysis as a filter. For the sensitivity  
17 of the vertical acceleration PSD to the connection parameters, the differential sensitivity method  
18 was adopted as Equation (5.2)

$$19 \quad \varepsilon_i = \frac{\Delta S_{out}(\alpha_i, \omega)}{\Delta \alpha_i}, \quad i = 1, 2, \dots, n \quad (5.2)$$

20 The differential step used was 0.001 times the mean value. The sensitivities of the vehicle body  
21 acceleration PSD to the primary and secondary stiffness and damping were calculated. The  
22 nondimensionalized sensitivities are shown in Figure 3. It can be seen that the sensitivity curves  
23 change with frequency. The sensitivities can be positive or negative, so that the influence of the  
24 response may be increased or reduced. Figure 3 shows that the system is most sensitive to  
25 secondary damping  $c_c^i$  and primary stiffness  $k_t^i$ , and so in the following the focus is on their  
26 uncertainty propagation.



1

2

Figure 3. 1-order differential sensitivities of acceleration PSD to the connection parameters for locations I and III.

3

## 4 5.2 Quantitative analysis of impact on vehicle body vibration of different uncertain 5 parameters

6

7

8

9

10

11

12

13

14

15

16

17

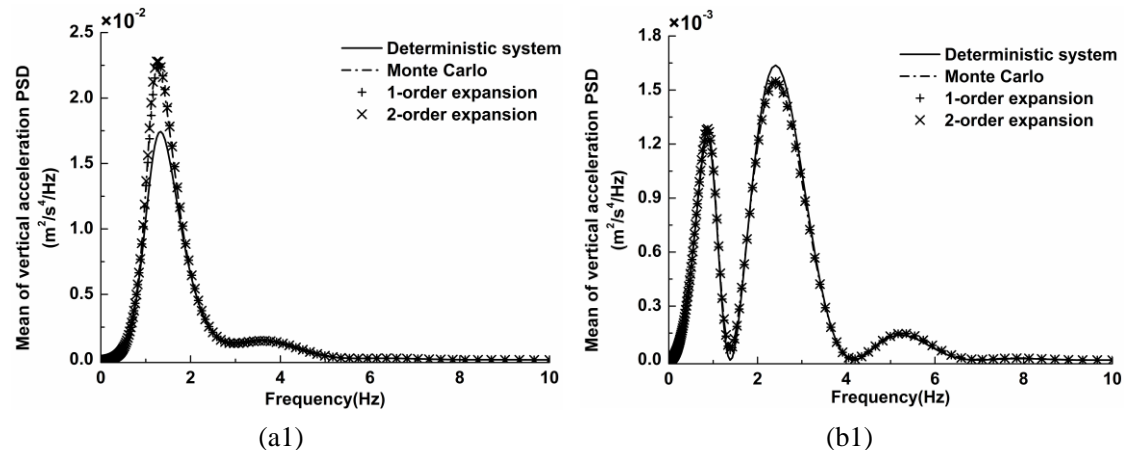
18

19

20

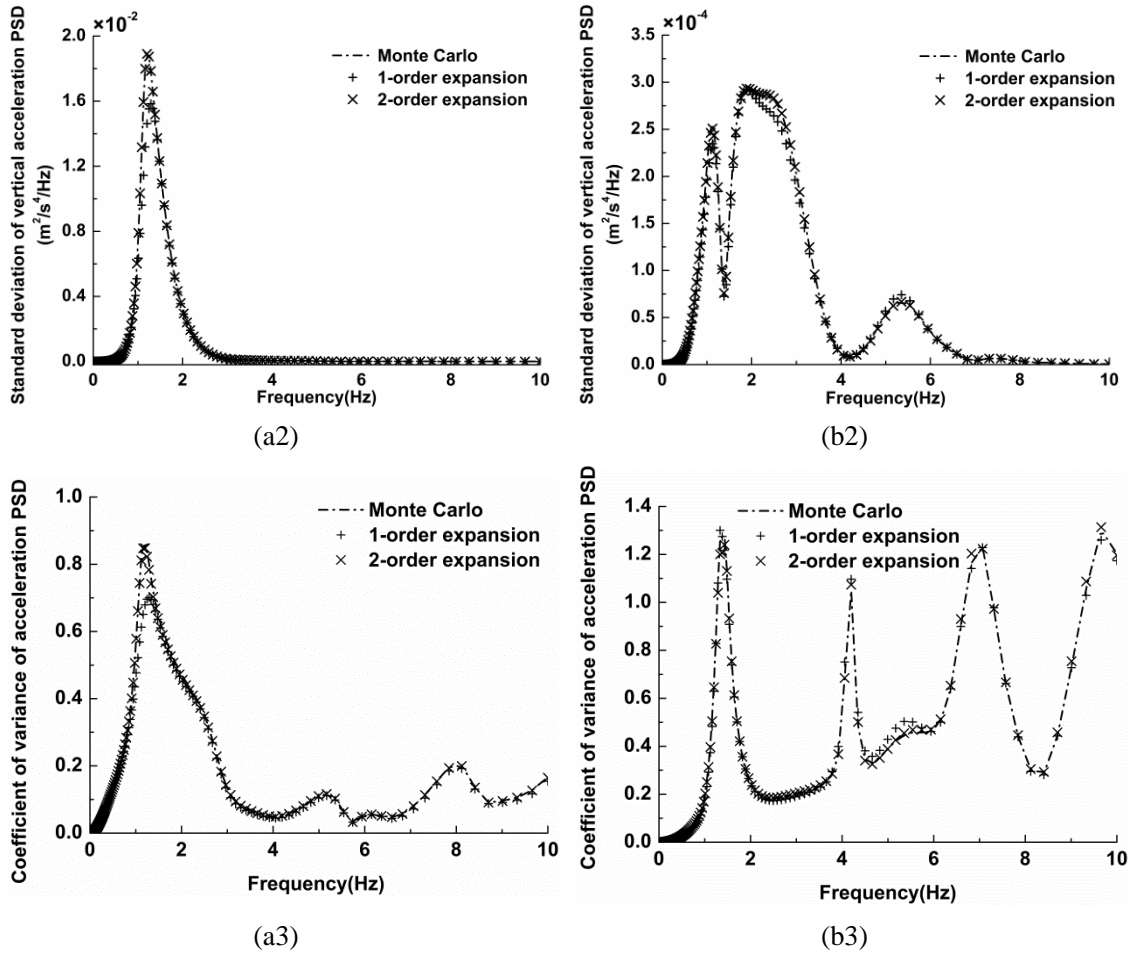
21

22



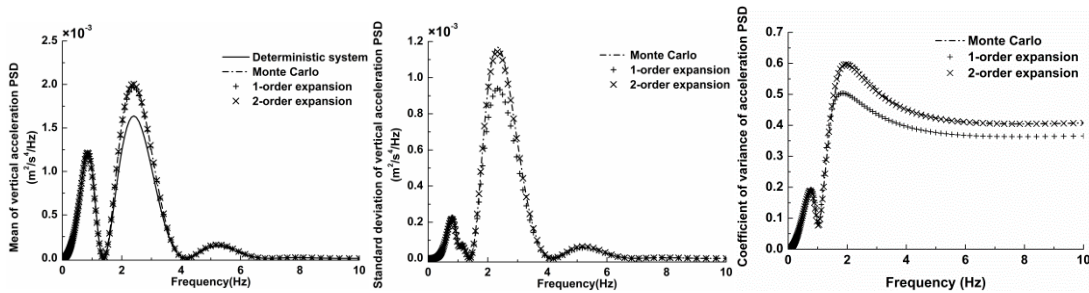
(a)

(b)



1 Figure 4. Mean, SD and CV of acceleration PSD for (a) location I when  $c_c^i$  is uncertain and (b) location III when  
 2  $k_t^i$  is uncertain.

3  
 4 On the other hand, the impacts of uncertain inertia parameters of the system on the vibration were  
 5 also investigated. It turns out that the impact of inertia parameter uncertainty to vibration response  
 6 is largely local, *i.e.* it affects the corresponding degree of freedom, but has little effect on others.  
 7 Only the vehicle body response is of concern, so considering the uncertainty of the inertia  
 8 parameters of the vehicle body, *i.e.*  $M_c$  and  $J_c$ , the mean, SD and CV of the vertical acceleration  
 9 PSD of location III are given in Figure 5, which shows that the uncertainty of the vehicle body  
 10 inertia parameter has a great influence on the acceleration PSD at location III, exceeding that of  
 11 uncertainty of  $k_t^i$ .



12 Figure 5. Mean, SD and CV of acceleration PSD for location III when  $M_c$  and  $J_c$  are uncertain.

13  
 14  
 15 To verify the correctness of the proposed method, comparison is made with direct Monte Carlo

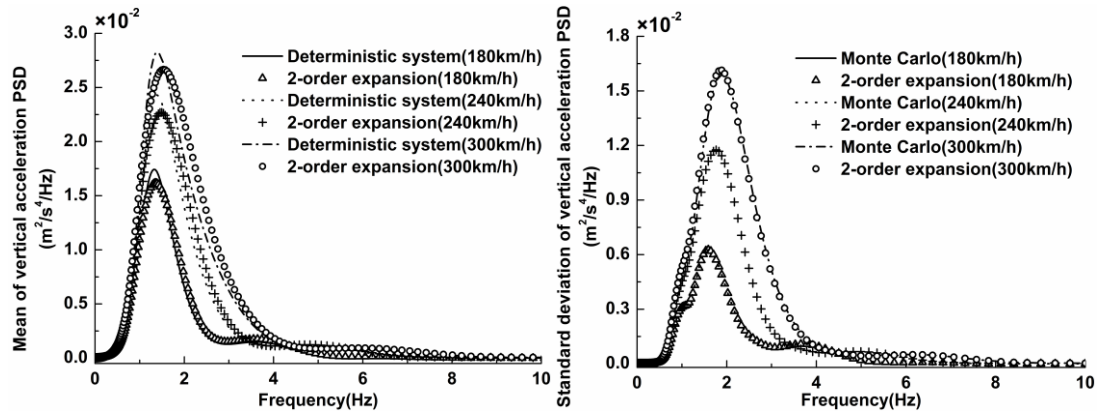
1 results. Figure 4 and 5 show the results of direct Monte Carlo simulation using 1000 samples,  
 2 including the statistical analysis of the first two order moments. It can be seen that the 1-order  
 3 moment can agree well when the random variables take the 1-order orthogonal expansion;  
 4 meanwhile, 2-order orthogonal expansion can satisfy the accuracy of 2-order moment. It turns out  
 5 that the 2-order expansion agrees well with Monte Carlo simulation even when the peak of CV of  
 6 response is close to 1. Monte Carlo simulation needs to establish and solve the equation repeatedly.  
 7 To ensure accuracy, the sample size is considerable, so that it is very time consuming. Instead the  
 8 proposed method expands the pseudo response in polynomial space. The original random system  
 9 dynamics equation converts into the expanded deterministic equation by using the orthogonality  
 10 and recursiveness of the polynomials. The projection in polynomial space is obtained by solving  
 11 the expanded deterministic equation only once, then the uncertain response is quantified by using  
 12 the effective uncertainty polynomial chaos expansion prediction model, see Equation (4.19). The  
 13 CPU times of the two methods are compared in Table 3 to show that the proposed method is much  
 14 more efficient than Monte Carlo simulation.

$k_t^i$ uncertain (4 variables)			$c_c^i$ uncertain (2variables)		
Monte Carlo	1-order	2-order	Monte Carlo	1-order	2-order
538.16s	4.68s	23.39s	554.29s	1.46s	2.36s

Table 3 Comparison of CPU time between methods

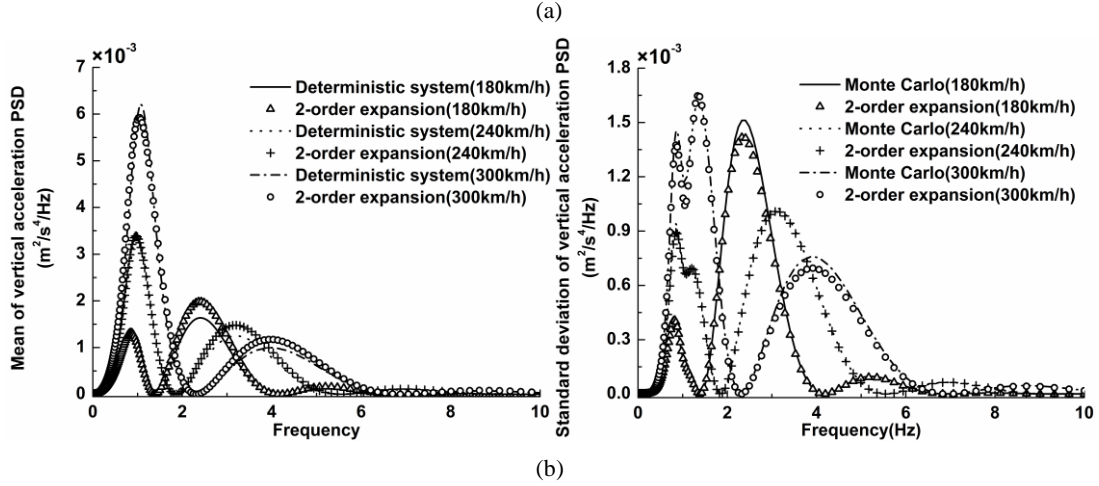
### 5.3 Random vibration analysis of uncertain coupled system at different velocities

19 The velocity  $v$  of the train is an important factor which influences the coupled system response  
 20 and so the results given in Figure 6 were obtained by using the hybrid pseudo excitation  
 21 polynomial chaos expansion (PEM-PCE) method for velocities of 180km/h, 240km/h and  
 22 300km/h. Combined with the discussion in the previous section, it can be seen that  $c_c^i$ ,  $k_t^i$ ,  $M_c$   
 23 and  $J_c$  are important when calculating the response of the uncertain coupled vehicle-rack system  
 24 under the track irregularity. Figure 6 shows the mean and SD of the acceleration PSD for locations  
 25 I and III for different velocities. It can be seen that when the velocity increases, the peak and shape  
 26 of the PSD curve are changed. This is mainly due to the phase lag between the four wheels  
 27 changing significantly as the velocity increases. It can also be seen that the difference between the  
 28 mean of uncertain response and the deterministic system response is approximately independent of  
 29 velocity. This can be explained by the fact that the system parameter uncertainty and the track  
 30 irregularity random excitation are independent.



31

1



2

3

4 Figure 6. Mean and SD of acceleration PSD for (a) location I and (b) location III for different velocities

5

when  $k_t^i$ ,  $c_c^i$ ,  $M_c$  and  $J_c$  are all uncertain.6 **5.4 Impact of uncertain parameter on the stability index**

7

8

9

10

11

12

13

According to the aforementioned analysis for random vibration responses with respect to the uncertain parameters, it can be seen that secondary damping  $c_c^i$ , primary stiffness  $k_t^i$  and the vehicle body inertias  $M_c$  and  $J_c$  are the most important parameters for the random vibration analysis of the uncertain system. Therefore, we must consider these uncertain parameters in combination in analysis when assessing running stability. The Chinese Railway vehicle dynamic performance evaluation and test specification (GB5599-85, 1985) for evaluation of train running stability was selected. The corresponding index is

14

$$W = 7.08 \left[ \int_{0.5}^{80} \left( \frac{F(f)}{f} \right)^{\frac{2}{3}} G(f) df \right]^{3/20} \quad (5.3)$$

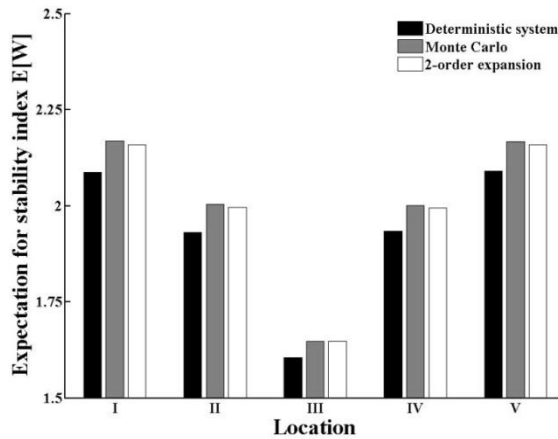
15

16

where  $G(f)$  is the power spectral density of acceleration,  $f$  is the frequency in Hz and  $F(f)$  is the frequency correction factor, with

17

$$F(f) = \begin{cases} 0.325f^2 & 0.5 \leq f \leq 5.9 \\ 400/f & 5.9 < f < 20 \\ 1 & f \geq 20 \end{cases} \quad (5.4)$$

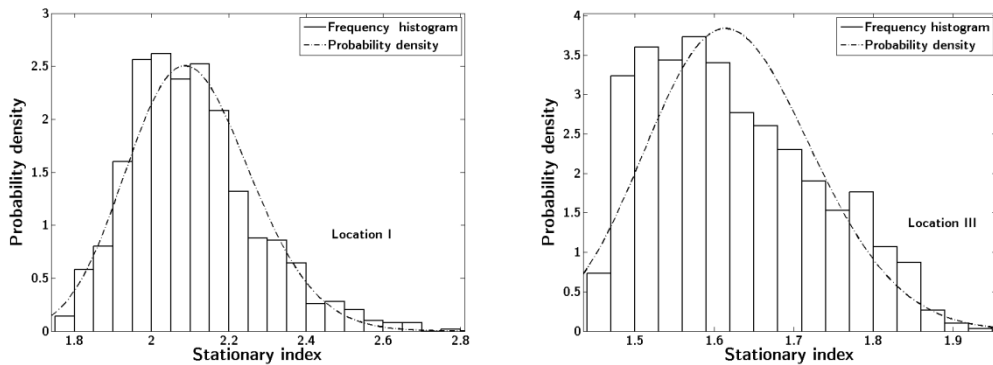


18

19

Figure 7. The mean of the stochastic stability index at different locations

1 Figure 7 shows the expectation for the stability index at different locations. Clearly the stability  
 2 index at all locations is higher than predicted by the deterministic system and although they all  
 3 achieve the standard (*i.e.* they are lower than 2.5), neglect of the parameter uncertainty will lead to  
 4 potentially risky analysis results. In addition, comparing the stability index at different locations  
 5 shows that it is lowest in the middle and highest at the ends. Locations I and III are respectively  
 6 the worst and the optimum location for the stability index, as investigated below. The mean and  
 7 variance of the stability at location I are 2.104 and 0.026, and at location III they are 1.624 and  
 8 0.011. The PDF of the random stability index was also investigated by taking the log likelihood  
 9 function value as the standard and selecting the inverse Gaussian distribution to fit the PDF. This  
 10 better reflects the overall probability characteristics, as shown in Figure 8. Further analysis  
 11 showed that the stability index at location I has a 98.94% probability of being less than 2.5, and  
 12 the stability index at location III has a 94.89% probability of being less than 1.8. The probability  
 13 distribution of the stability index provides a good indicator when performing reliability analysis.



14  
 15 Figure 8. Probability density fitting of the stability index at locations I and III.

16  
 17 **6 Conclusions**

18 A new effective assessment method has been developed for random vibration of an uncertain  
 19 coupled vehicle-track system under track irregularity. The dynamic equation of coupled  
 20 vehicle-track systems under mixed physical coordinates and dual coordinates has been established  
 21 in the framework of the Hamiltonian system, and the governing equation with respect to the  
 22 uncertain parameters has been derived by using orthogonal polynomials for the dynamic analysis  
 23 of coupled systems. An assessment of random vibration with respect to the uncertain parameters  
 24 has been established for the coupled vehicle-track system by using the pseudo-excitation method.  
 25 Numerical results show that the established method has high accuracy and that this work provides  
 26 an effective means for solving practical engineering problems that involve the uncertainty of  
 27 vehicle-track systems.

28 **References**

29 Borwein, P.B. and Erdélyi, T. (1995), *Polynomials and Polynomial Inequalities*. Springer , New York.  
 30 Cameron, R.H. and Martin, W.T. (1947), “The orthogonal development of non-linear functionals in series of Fourier-Hermite  
 31 functionals”, *Annals of Mathematics*, Vol. 48, pp. 385-92.  
 32 Caprani C.C. (2014), “Application of the pseudo-excitation method to assessment of walking variability on footbridge vibration”,  
 33 *Computers & Structures*, Vol. 132, pp. 43-54.

1 Chang, T.P., Lin, G.L. and Chang, E. (2006), "Vibration analysis of a beam with an internal hinge subjected to a random moving  
2 oscillator", *International Journal of Solids and Structures*, Vol.43, pp. 6398-412.

3 Clough, R.W. and Penzien, J. (1975), *Dynamics of Structures*, McGraw-Hill, New York.

4 D'Aveni, A., Muscolino, G. and Ricciardi, G. (1996), "Stochastic analysis of a simply supported beam with uncertain parameters  
5 subjected to a moving load", *Structural Dynamics: EURO-DYN'96*, Florence, Italy: 439-46.

6 De Rosa, S., Franco F. and Ciappi E. (2015), "A simplified method for the analysis of the stochastic response in discrete  
7 coordinates", *Journal of Sound and Vibration*, Vol. 339: pp. 359-75.

8 Garg, V.K. and Dukkipati, R.V. (1984), *Dynamics of Railway Vehicle Systems*, Academic Press, New York.

9 GB5599-1985: Railway vehicle-Specification for evaluation the dynamic performance and accreditation test. 2-3.

10 Ghanem, R.G. and Kruger, R.M. (1996), "Numerical solution of spectral stochastic finite element systems", *Computer Methods  
11 in Applied Mechanics and Engineering*, Vol.129, pp. 289-303.

12 Ghanem, R.G. and Red-Horse, J. (1999), "Propagation of probabilistic uncertainty in complex physical systems using a  
13 stochastic finite element approach", *Physica D: Nonlinear Phenomena*, Vol. 133, pp. 137-44.

14 Ghanem, R.G. and Spanos, P.D. (1991), *Stochastic finite elements: a spectral approach*, Springer-Verlag, New York.

15 Gładysz, M. and Śniady, P. (2009), "Spectral density of the bridge beam response with uncertain parameters under a random train  
16 of moving forces", *Archives of Civil and Mechanical Engineering*, Vol. 9, pp.31-47.

17 Iwnicki, S. (2006), *Handbook of Railway Vehicle Dynamics*, CRC Press, Boca Raton.

18 Kewlani, G., Crawford, J. and Iagnemma, K. (2012), "A polynomial chaos approach to the analysis of vehicle dynamics under  
19 uncertainty", *Vehicle System Dynamics*, Vol. 50, pp. 749-74.

20 Lin, J.H. (1992), "A fast CQC algorithm of PSD matrices for random seismic responses", *Computers and Structure*, Vol. 44, pp.  
21 683-87.

22 Lin, J.H., Fan, Y., Bennett, P.N. and Williams, F.W. (1995), "Propagation of stationary random waves along substructural chains",  
23 *Journal of Sound and Vibration*, Vol. 180, pp. 757-67.

24 Lin, J.H., Zhang Y.H. and Zhao Y. (2011), "Pseudo excitation method and some recent developments", *Procedia Engineering*,  
25 Vol. 14, pp. 2453-8.

26 Lin J.H., Zhang Y.H. and Zhao Y. (2014), "Seismic random response analysis", Chen W.F. and Duan L.(Ed.), *Bridge Engineering  
27 Handbook*, CRC Press, Boca Raton, pp. 133-62.

28 Lin, J.H., Zhao, Y. and Zhang, Y.H. (2001), "Accurate and highly efficient algorithms for structural stationary/non-stationary  
29 random responses", *Computer Methods in Applied Mechanics and Engineering*, Vol. 191, pp. 103-11.

30 Muscolino, G., Benfratello, S. and Sidoti, A. (2002), "Dynamics analysis of distributed parameter system subjected to a moving  
31 oscillator with random mass, velocity and acceleration", *Probabilistic engineering mechanics*, Vol. 17, pp. 63-72.

32 Thompson, D.J. (1993), "Wheel-rail noise generation, part IV: contact zone and results", *Journal of Sound and Vibration*, Vol.  
33 161, pp. 447-66.

34 Wiener, N. (1938), "The homogeneous chaos", *American Journal of Mathematics*, Vol. 60, pp. 897-936.

35 Wu, S.Q. and Law, S.S. (2010), "Dynamic analysis of bridge-vehicle system with uncertainties based on the finite element  
36 model", *Probabilistic Engineering Mechanics*, Vol. 25, pp. 425-32.

37 Wu, S.Q. and Law, S.S. (2011), "Dynamic analysis of bridge with non-Gaussian uncertainties under a moving vehicle",  
38 *Probabilistic Engineering Mechanics*, Vol. 26, pp. 281-93.

39 Xiu, D. (2010), *Numerical Methods for Stochastic Computations: A Spectral Method Approach*, Princeton University Press,  
40 Princeton.

41 Xiu, D. and Karniadakis, G.E. (2002), "The Wiener-Askey polynomial chaos for stochastic differential equations", *SIAM Journal  
42 on Scientific Computing*, Vol. 24, pp. 619-44.

43 Yu, L. (2010), *Fatigue Reliability of Ship Structures*, PhD thesis, University of Glasgow, Glasgow.

44 Zhang, W.S. and Xu Y.L. (1999), "Dynamic Characteristics and seismic response of adjacent buildings linked by discrete

- 1 dampers”, *Earthquake Engineering and Structural Dynamics*, Vol. 28, pp. 1163-85.
- 2 Zhang, Y.W., Lin, J.H., Zhao, Y., Howson, W.P. and Williams, F.W. (2010), “Symplectic random vibration analysis of a vehicle
- 3 moving on an infinitely long periodic track”, *Journal of Sound and Vibration*, Vol. 329, pp. 4440-54.
- 4